

## Portland State University PDXScholar

---

Civil and Environmental Engineering Faculty  
Publications and Presentations

Civil and Environmental Engineering

---

11-1-2009

# Particle Resuspension in the Columbia River Plume Near Field

Emily Y. Spahn  
*Portland State University*

Alexander R. Horner-Devine  
*University of Washington*

Jonathan Nash  
*Oregon State University*

David A. Jay  
*Portland State University*

Levi Kilcher  
*Oregon State University*

Let us know how access to this document benefits you.

Follow this and additional works at: [https://pdxscholar.library.pdx.edu/cengin\\_fac](https://pdxscholar.library.pdx.edu/cengin_fac)

 Part of the [Civil and Environmental Engineering Commons](#)

---

### Citation Details

Spahn, E. Y., A. R. Horner-Devine, J. D. Nash, D. A. Jay, and L. Kilcher (2009), Particle resuspension in the Columbia River plume near field, *J. Geophys. Res.*, 114, C00B14.

This Article is brought to you for free and open access. It has been accepted for inclusion in Civil and Environmental Engineering Faculty Publications and Presentations by an authorized administrator of PDXScholar. For more information, please contact [pdxscholar@pdx.edu](mailto:pdxscholar@pdx.edu).



## Particle resuspension in the Columbia River plume near field

Emily Y. Spahn,<sup>1</sup> Alexander R. Horner-Devine,<sup>1</sup> Jonathan D. Nash,<sup>2</sup> David A. Jay,<sup>3</sup> and Levi Kilcher<sup>2</sup>

Received 27 June 2008; revised 9 June 2009; accepted 30 July 2009; published 24 November 2009.

[1] Measurements of suspended sediment concentration, velocity, salinity, and turbulent microscale shear in the near-field region of the Columbia River plume are used to investigate the mechanisms of sediment resuspension and entrainment into the plume. An east-west transect was occupied during spring and neap tide periods in August 2005 and May 2006, corresponding to low and high river discharge conditions, respectively. During the high-discharge period the plume is decoupled from the bottom, and fine sediment resuspended from the bottom does not leave the benthic boundary layer. The primary modes of sediment transport associated with the plume are advection of sediment from the estuary and removal of sediment from the plume by gravitational settling and turbulent mixing. In contrast, the plume is much less stratified during low-discharge conditions, and large resuspension events are observed that entrained sediment through the water column and into the plume. Our measurements indicate that two factors control the magnitude and timing of sediment resuspension and entrainment: the supply of fine sediment on the seabed and the relative influence of tidal turbulence compared with buoyancy input from the river. The latter is quantified in terms of the estuary Richardson number  $Ri_E$ . The magnitude of vertical turbulent sediment flux is correlated with  $Ri_E$  during the low-flow period when there is a sufficient supply of bottom sediment in the near-field region. Such sediment resuspension may be an important mechanism for the delivery of bioavailable micronutrients to the plume during the summer.

**Citation:** Spahn, E. Y., A. R. Horner-Devine, J. D. Nash, D. A. Jay, and L. Kilcher (2009), Particle resuspension in the Columbia River plume near field, *J. Geophys. Res.*, *114*, C00B14, doi:10.1029/2008JC004986.

### 1. Introduction

[2] Rivers are the dominant source of freshwater, and dissolved and particulate matter to the ocean [McKee *et al.*, 2004; Dagg *et al.*, 2004]. Globally, rivers discharge approximately  $10^6 \text{ m}^3 \text{ s}^{-1}$  of water to the ocean per year, while transporting up to 20 billion metric tons of sediment [Milliman and Syvitski, 1992]. The fate and impact of riverine sediments depends on transport processes and transformations in rivers, estuaries and the coastal ocean, and buoyant plumes are the locus of rapid transformation of terrestrial materials entering the ocean [Dagg *et al.*, 2004]. Whether sediment particles entering coastal waters are incorporated into the coastal ecosystem, buried on the shelf or transported to the deep ocean depends to a large degree on the rate at which they are removed from the plume and if, or when, they are resuspended from the bottom.

[3] River-derived shelf sediments are an important source of micronutrients to the coastal ecosystem. For example, iron

can be a limiting factor on phytoplankton primary productivity in the California Current System (CCS) along the U.S. west coast, where coastal upwelling typically provides high concentrations of nitrate and silicic acid [Bruiland *et al.*, 2001]. Johnson *et al.* [1999] show that the primary source of dissolvable iron to the CCS is resuspension of benthic particles, which are subsequently carried to the surface by coastal upwelling, rather than directly supplied from rivers. Rivers are generally thought to contribute only a fraction of the iron that they carry to the coastal ocean due to trapping in estuaries by flocculation and settling [e.g., Boyle *et al.*, 1977]. Chase *et al.* [2007] suggest that the origin of coastal iron is somewhat more complex, however. Based on an analysis of coastal waters along the west coast of North America, they show that phytoplankton biomass is elevated in regions with high river discharge. They attribute this trend to wintertime iron input from rivers, which bypasses the estuaries and is stored on the shelf. The shelf sediment and iron is then resuspended in summer months and fuels coastal productivity. Their hypothesis requires that iron is exported more effectively from the estuary during high river flow conditions. This assumption is consistent with recent findings by Bruiland *et al.* [2008] for the Columbia River near field, who find that the contribution of iron to the plume from the estuary is higher during high river discharge conditions in May 2006 compared with periods of lower discharge. Johnson *et al.* [1999] show that diffusion from the bottom boundary layer is

<sup>1</sup>Department of Civil and Environmental Engineering, University of Washington, Seattle, Washington, USA.

<sup>2</sup>College of Oceanic and Atmospheric Sciences, Oregon State University, Corvallis, Oregon, USA.

<sup>3</sup>Department of Civil and Environmental Engineering, Portland State University, Portland, Oregon, USA.

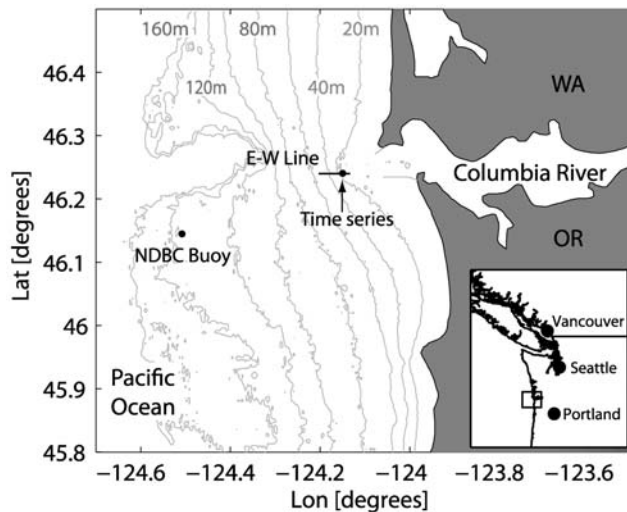


**Figure 1.** Columbia River mouth map. The east-west transect line (EW), which is indicated by the thick black line, begins 4.5 km from the mouth of the river on the main axis of the plume and extends to 9 km from the mouth. The location of the near-field time series is marked by a dot and is approximately 5.5 km from the river mouth.

not sufficient to provide the observed concentration of iron to the upwelling system and conclude that flux of iron from shelf sediment deposits must be due to sediment resuspension. However, the range of mechanisms that result in sediment resuspension from the shelf have not been completely identified.

[4] Previous observations of sediment resuspension in shelf systems have been associated with internal waves [Bogucki *et al.*, 1997], tidal currents [Souza *et al.*, 2004], anthropogenic stresses [Tragou *et al.*, 2005] and wave stresses [e.g., Wiberg *et al.*, 1994]. In river-influenced shelf regions a number of additional mechanisms exist that may cause resuspension such as energetic plume fronts [Orton and Jay, 2005], plume-front-generated internal waves [Nash and Moum, 2005] and amplified tidal flows from the estuary. In general, resuspension is expected within the frontal or lift-off zone, which encompasses the vertically well-mixed bottom-attached region and typically extends to a water depth of approximately 10 m [Geyer *et al.*, 2004]. Seaward of the frontal region the plume becomes more strongly stratified and detaches from seabed. The location and width of the frontal region is a complex function of the density stratification, outflow velocity, tidal currents and bottom slope.

[5] During the River Influences on Shelf Ecosystems (RISE) project large sediment resuspension events were observed in spring and late summer in the near-field region of the Columbia River plume seaward of the location where plume lift-off is typically observed. The location and extent of these events suggest that they are capable of generating a significant flux of sediment from the seabed to the surface plume. To quantify this resuspension and elucidate its seasonal variability, we compare observations from two cruises: one in the spring and one in late summer. By combining detailed measurements of the turbulence field with synchronous and colocated measurements of suspended sediment concentration throughout the water column, we are able to make direct estimates of vertical turbulent sediment fluxes

with unprecedented spatial and temporal resolution. In the winter, storms likely cause significant wave-generated resuspension [Nittrouer and Sternberg, 1981]. During the more biologically active summer season, however, wave activity is much lower and resuspension due to the processes described here may generate an important flux of sediment and micro-nutrients to the plume.

[6] The objectives of this work are to investigate the interplay between resuspension, deposition, and horizontal advection in the plume near field during the spring-summer periods considered in the RISE project. In particular, we seek to determine how these processes vary with river flow and tidal forcing. Finally, by relating sediment resuspension to buoyancy input and tidal current magnitude we hope to provide a framework for understanding the conditions leading to input of bottom sediments into the plume that can be applied more generally to the Columbia plume and to other plume systems.

## 2. Setting and Conditions

[7] The Columbia ranks eighteenth among world rivers as a source of freshwater, but its sediment discharge is comparatively low for a river of its size [McKee *et al.*, 2004; Bottom *et al.*, 2005]. It presently discharges about 8 million tons of sediment each year, down from about 20 million tons per year before installation of the reservoir system. The present sediment discharge includes  $\sim 5$  million tons of fines, most of which escapes to the ocean, and  $\sim 3$  million tons of sand, little of which reaches the ocean. The fate of the sediment supplied to the shelf is less clear. Fines are believed to be deposited near the coast in spring and summer. Winter storms act to resuspend and move bottom sediments away from the coast to a midshelf silt deposit [Nittrouer and Sternberg, 1981; Wright and Nittrouer, 1995]. During winter freshets, at least some of the fine material may bypass the inner shelf and move quickly offshore. Regardless of the timing of supply to the inner shelf, observations described below suggest that plume-related resuspension occurs during summer, even in the absence of storms. While resuspension in the near-field plume during summer is not likely to transport a large mass of sediment, it may contribute benthic particle-associated nutrients to the plume ecosystem during a period when they can have a substantial impact.

[8] The Columbia River flows into the Pacific Ocean along the border between Washington and Oregon, USA (Figure 1). The coastal waters of the Washington and Oregon shelf form a highly productive ecosystem due in large part to the strong upwelling-driven supply of nutrient rich deep water. Despite the fact that upwelling wind stress is higher off the Oregon coast than the Washington coast, chlorophyll levels are observed to be higher to the north [Landry *et al.*, 1989]. One of the objectives of the RISE project, a 5 year interdisciplinary study of the Columbia plume, was to explain this apparent paradox. A central hypothesis of the project is that the Columbia plume, which influences the Washington shelf preferentially, is a major cause of the discrepancy in observed productivity. Indeed, plume waters have elevated chlorophyll concentrations of up to  $20 \mu\text{g/l}$  [Landry *et al.*, 1989]. These high chlorophyll concentrations occur despite the fact that the Columbia (unlike most large rivers) does not provide large amounts of nitrate to coastal waters [Conomos *et al.*, 1972;

*Sullivan et al.*, 2001]. However, the Columbia can provide high concentrations of silicic acid and the micronutrients iron and manganese, which are important for supporting productivity in coastal waters. These constituents typically enter the system from upstream, either in dissolved form or adsorbed onto river sediment. Observations from the July 2004 RISE cruise confirm that the river water is rich in all three constituents [*Lohan and Bruland*, 2006; *Aguilar-Islas and Bruland*, 2006]. However, the pathway by which each constituent arrives and is distributed in the plume remains unclear.

[9] Transfer of sediment to the shelf from the Columbia River and estuary is influenced by, but does not precisely follow, the seasonality of the river flow. It occurs primarily under three circumstances [*Bottom et al.*, 2005; *Fain et al.*, 2001].

[10] 1. It occurs during the annual spring freshet in May and June. Before construction of the reservoir system, this period accounted for the bulk of the sediment transport in most years.

[11] 2. It occurs during brief winter floods (rain-on-snow events), when fine sediment concentrations in the river are greatly elevated relative to other times of year. Due to flow regulation by reservoirs since circa 1970, maximum winter flows have frequently been larger than spring freshet flows, so that the primary period of sediment supply may now be during the winter. This is particularly true for fines, whose supply to the river is sporadic, and occurs mostly in winter.

[12] 3. It occurs during spring tides for several months after any major supply event to the estuary.

[13] Export of river sediment to coastal waters is buffered by estuary processes and strongly influenced by tidal amplitude. The estuarine turbidity maxima (ETM) and peripheral bays of the estuary prolong the residence time of suspended particles in that region and provide an enhanced opportunity for flocculation. As tidal range increases toward a spring tide, the ETM is supplied with particles from peripheral areas. These particles are then exported to the shelf during the strongest ebbs. Further details of these complex exchanges are described by *Fain et al.* [2001].

[14] Studies in the Columbia ETM group the suspended particulate into four settling velocity classes: 0.014 (C1), 0.3 (C2), 2.0 (C3), and 14 mm s<sup>-1</sup> (C4) [*Reed and Donovan*, 1994; *Fain et al.*, 2001]. These settling classes are associated with clay to fine silt, medium to coarse silt, fine aggregate material, and sand and large aggregates, respectively, and account for 2.5%, 28.3%, 24.0%, and 45.2% by mass of the particles observed between May and December. Based on acoustic and optical backscatter measurements, *Fain et al.* [2001] conclude that the sand fraction (C4) is almost entirely retained in the estuary and that the silt (C2) and fine aggregate (C3) classes make up most of the particles exported from the estuary. Based on the estuary observations, exported particulate is divided approximately evenly by mass between particles with fall velocities of 0.3 mm s<sup>-1</sup> and 2.0 mm s<sup>-1</sup>. High concentrations of finer particles (C1) may be present sporadically during winter high-flow periods, but no such events were observed by *Fain et al.* [2001].

[15] The Columbia River receives a significant fraction of its flow from melting of winter snowpack, resulting in a strong seasonal cycle in the total discharge to the coastal ocean. Conditions during the summer (August 2005) and

spring (May 2006) cruises are presented in Figure 2. During the summer cruise the river discharge was approximately 3500–4500 m<sup>3</sup> s<sup>-1</sup>, but more than twice that value during the spring cruise (Figure 2a). This difference is expected due to spring melt from upstream snowpack. However, 2005 was also a relatively low flow year, whereas 2006 was close to normal [*Hickey et al.*, 2009].

[16] The suspended sediment concentration (SSC) in the river during 2005–2006 roughly followed the discharge turbidity measured 86 km upstream of the river mouth and was roughly twice as large in May 2006 compared to August 2005 (Figure 2b). However, the turbidity record is too far landward to reflect spring tide export events from the ETM that may have occurred in August 2005.

[17] Wind and wave data were acquired from the NOAA buoy located near the mouth of the Columbia River (Station 46029). Winds near the Oregon and Washington coasts are predominantly northward (downwelling favorable) during winter and southward (upwelling favorable) during the summer [*Hickey et al.*, 1998], though variability is high. The August 2005 cruise took place during a period of predominantly upwelling winds (Figure 2c); however, the middle part of the May 2006 cruise had unusually strong northward winds for late May. Wave stress was estimated from wave height and period using the formulation described by *Grant and Madsen* [1979]. Currents were not included in this estimate since current-generated bottom stress is measured using the microstructure profiler. Wave stresses are low between June and September in both years and peak during the winter months. The high-flow sampling in May 2006 was at the end of the stormy period and wave stresses were 2–3 times higher than during the August sampling.

### 3. Methods

[18] Repeated, rapidly executed surveys of turbulence, optics and acoustics were obtained aboard the R/V *Point Sur* in the near-field region of the Columbia River plume during 3 RISE cruises in 2004, 2005 and 2006. For this study, a detailed sediment dynamics data set was acquired during 5–26 August 2005 and 22–31 May 2006 using a combination of turbulence profiler data collected by OSU's Ocean Mixing Group and suspended sediment concentration data collected by UW.

#### 3.1. Instrumentation

[19] Full-depth profiles of salinity, temperature, optical backscatter (OBS), biological fluorescence and turbulence (microscale shear and temperature variance) were obtained using *Chameleon*, the OSU Ocean Mixing Group's loosely tethered microstructure profiler [*Moum et al.*, 1995]. The free-falling profiler was tethered to a free-spooling block on the ship's crane, so that profiles were obtained 5 m outboard of the ship's starboard quarter to avoid ship wake contamination. The configuration is described in greater detail by *Nash et al.* [2009]. The profiler was equipped with a bottom crasher, so scalar measurements were obtained continuously from the surface to within 10 cm from the bottom at a nominal 1 m s<sup>-1</sup> fall speed. Profiles were obtained every 1–3 min, providing 50–500 m horizontal resolution depending on ship speed (2–10 knots over ground) and water depth. Scalar and turbulence data were sampled at 51.2 and 204.8 Hz, respec-

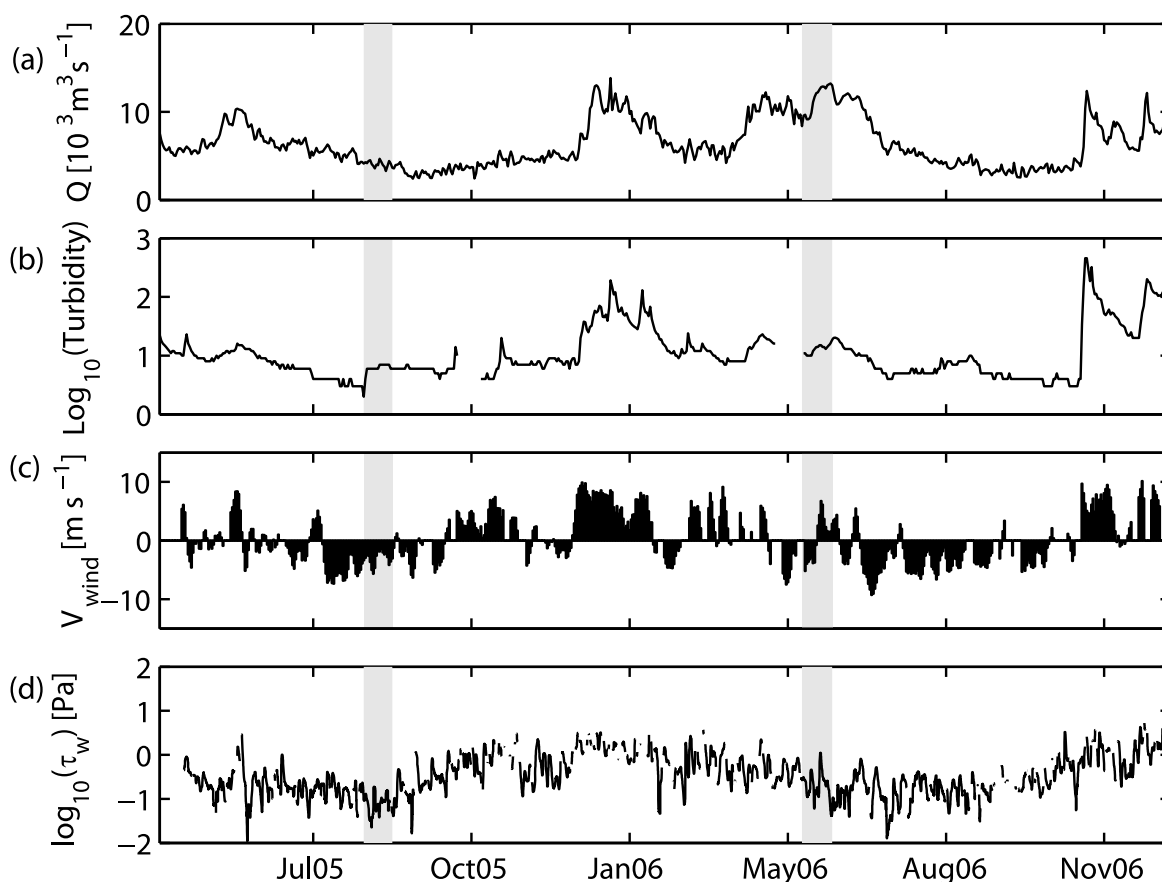


**Figure 2.** (a) River discharge and (b) turbidity measured 86 km upstream from the mouth of the Columbia River at the Beaver Army Terminal. (c) Alongshore wind speed (positive is northward) measured at the Columbia River bar buoy. (d) Estimated wave-generated bottom stress based on wave data from the Columbia River bar buoy. The shading indicates the low- and high-flow periods corresponding to the August 2005 and May 2006 cruises.

tively; profiler motion is measured using 3 component accelerometers sampled at 102.4–204.8 Hz. Optical backscatter was measured at 880 nm wavelength with a custom Seapoint Sensors turbidity meter (0.1 s time constant; <2% deviation from linearity over 0–750 FTU) sampled at 51.2 Hz. All data have been averaged into 1 m vertical bins in so that they are on a common grid.

[20] Water column velocities were measured using a pole-mounted 1200 kHz RD Instruments Acoustic Doppler Current Profiler (ADCP), with bottom tracking and 0.5 m vertical bins; the first bin is centered at 2.35 m. This was augmented with the shipboard 300 kHz data (1 m bins) for depths greater than  $\sim 20$  m.

### 3.2. Suspended Sediment Concentration

[21] To determine suspended sediment concentration (SSC) from Optical Backscatter (OBS) data, water samples were collected with Niskin bottles on the CTD rosette, filtered through preweighed 0.45 micron Millipore membrane filters and weighed to determine suspended sediment concentration. Approximately collocated and contemporaneous bottle samples and OBS measurements were used to generate a linear calibration for the OBS (Figure 3). Using a robust least squares fitting method, we obtain an  $r^2$  value of approximately 0.9 in both August and May.

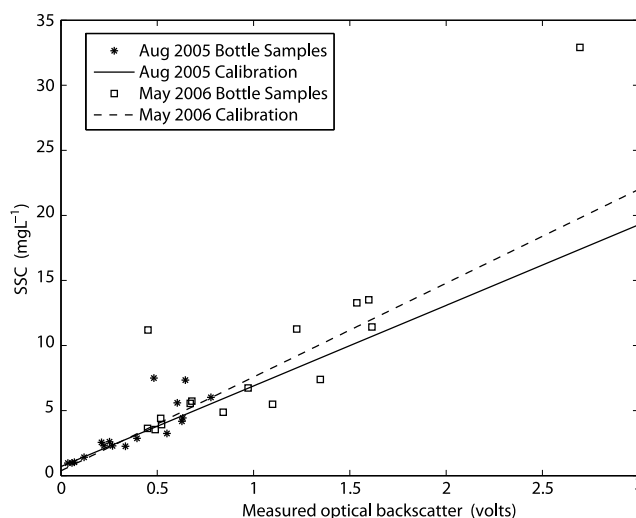


**Figure 3.** Measured suspended sediment concentrations from bottle samples versus approximately collocated measurements of optical backscatter. Solid and dashed lines are the relationships used for calibration of the August 2005 and May 2006 optical backscatter data, respectively.

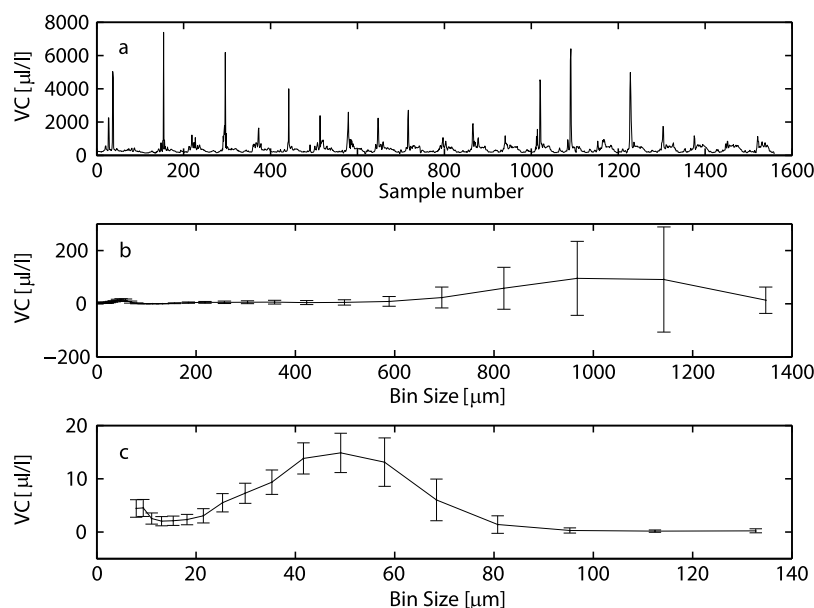


**Figure 4.** (a) Particle volume concentrations from the LISST-FLOC as it was undulated through the plume in June 2005. (b) Particle size distribution for the entire size range, showing a peak in concentration and noise at 1 mm sizes that is presumed to be due to contamination from density stratification. (c) Particle size distribution in the silt size range, showing a peak at 50  $\mu\text{m}$ .

### 3.3. Fall Velocity

[22] We deployed a LISST (laser in situ scattering and transmissometry) instrument on the ship's CTD frame to measure particle size distribution and volume concentration. However, a large fraction of these data were contaminated, as the LISST optics are sensitive to the change in index of refraction in highly stratified environments like that of the Columbia River plume [Styles, 2006; Mikkelsen et al., 2008]. The stratification appears in the LISST data as an increased number of large particles.

[23] The fall velocity ( $w_s$ ) was estimated using two separate methods and is compared with values from other plume systems and the Columbia estuary. The first method was developed and used for the 2004 cruise, using Niskin bottles to estimate fall velocity [Chisholm and Jay, 2004]. Four samples from within the plume region were selected from the 2004 cruise, giving a fall velocity estimate of  $0.3 \pm 0.15 \text{ mm s}^{-1}$ . This method is only useful during calm periods without significant vessel heave; it was not repeated during subsequent cruises.

[24] The second method involved choosing periods within the LISST record in which contaminated data could be separated from the good data. This is possible when the stratification is weak enough that it only contaminates the particle size bins that are significantly larger than the actual particle size. The record of measured volume concentration, VC, in the plume during a June 2005 cruise is shown in Figure 4a. These data were acquired when the LISST instrument was undulated in the plume near the surface, causing VC to increase and decrease as the instrument comes in and out of the plume. Spikes are evident in the data, presumably due to the effect of stratification as the instrument enters more stratified regions of the plume. As observed in the particle size distribution, these spikes contaminate the measurements of volume concentration primarily for the

large particle sizes (Figure 4b). They do not appear to affect the particle size distribution for the low particle sizes, however (Figure 4c). Analysis of the uncontaminated band resulted in an estimate of the average particle size of 50  $\mu\text{m}$  and the average volume concentration of  $80 \text{ ml l}^{-1}$ . Following the method of Mikkelsen and Pejrup [2001] and using a typical mass concentration in the plume of  $10 \text{ mg l}^{-1}$ , the density anomaly associated with the particles is  $125 \text{ kg m}^{-3}$ . This gives an estimate of approximately  $0.2 \text{ mm s}^{-1}$  for the fall velocity, consistent with the settling tube method.

[25] The fall velocity estimate of  $w_s = 0.3 \text{ mm s}^{-1}$  is consistent with values from Hill et al. [2000], who report values for the settling velocity of partially flocculated sediments in the Eel river plume of  $0.1 \text{ mm s}^{-1}$ . One notable difference between the Columbia and Eel plume systems is the existence of the large Columbia River estuary. As described in section 2, the estuary provides an enhanced opportunity for flocculation, which may result in an increased settling rate. The above fall velocity estimate is consistent with the silt settling class observed in the Columbia estuary [Reed and Donovan, 1994; Fain et al., 2001]. For this work we assume that the fall velocity is  $w_s = 0.3 \text{ mm s}^{-1}$ ; however, we also include calculations based on the aggregate fall velocity class  $w_s = 2.0 \text{ mm s}^{-1}$ , which likely represents an upper bound on the fall velocity observed in the near-field plume region.

### 3.4. Turbulent Flux Measurements

[26] Turbulence data were computed in 1 m vertical bins following the procedures outlined in the work by Moum et al. [1995]. TKE dissipation rate  $\varepsilon$  was computed assuming isotropic turbulence and integrating shear variance in the dissipation subrange from two orthogonal airfoil shear probes (providing  $du/dz$  and  $dv/dz$ ). The turbulent diffusivity  $K_p$  is computed from  $\varepsilon$  assuming a TKE production-dissipation

balance [Osborn, 1980]. For regions of low  $N^2$  the Osborn method fails and  $K_\rho$  is not estimated. The bottom stress  $\tau_b$  is computed from profiles of  $\varepsilon$  in the bottom boundary region to determine  $u_*$  using the dissipation method described by Perlin *et al.* [2005].

[27] Turbulence may resuspend sediment from the bottom and mix it up into the water column. The vertical turbulent sediment flux  $F_t$  can be estimated by combining the vertical gradient in the measured suspended sediment concentration field  $C$  acquired with the calibrated OBS and the diffusivity based on the turbulence measurements:

$$F_t = K_\rho \frac{dC}{dz}.$$

[28] Absent any means of measuring the sediment diffusivity  $K_{sed}$  directly, we assume that it is equal to the scalar diffusivity  $K_\rho$ , or,  $\beta = K_{sed} K_\rho^{-1} = 1$ . This may be a poor assumption for heavy particles when the particle's inertia causes  $K_{sed}$  to exceed  $K_\rho$  [van Rijn, 1984]. An assumption that  $\beta = 1$  is justified for fine sediment and aggregate particles carried in the plume and deposited on the seabed, but not the sand particles that makeup the remainder of the seabed [van Rijn, 1984; Rose and Thorne, 2001]. Our observations indicate that the bottom stresses are only just sufficient to initiate motion in sand particles under peak stresses and we conclude that sand makes up little to none of the resuspended material that we observe higher in the water column.

### 3.5. Sampling

[29] In this analysis, we focus on data that were collected along an across-shelf (EW) sampling line located between 124.13 and 124.21°W at the latitude of the Columbia River mouth, 46.24°N (Figure 1). The line begins approximately 4.5 km from the river mouth and extends 4.5 km west along the main axis of the outflow from the estuary. It took between 45 and 120 min to cover the transect, depending primarily on the strength of the opposing tidal current. The data set includes 33 transects during spring tide on 29 May 2006, and 123 on 20 August 2005. During neap tides, 83 transects were completed on 10 August and 12 in May. Operations along the line during neap tide in May were abandoned due to stormy weather. As discussed in section 4.5, this period is likely to have been important in terms of sediment resuspension and transport, but could not be sampled due to safety concerns. Continuous sampling spanned at least 1 day for all four periods, except the neap period in May 2006. We consider in detail data from five transects during spring tide peak ebb in the high- and low-flow periods. These are chosen because they correspond to periods of high export of sediment from the estuary and tidally generated bottom stress. Sampling on a north-south transect resulted in additional samples at the intersection of that line and the EW line. We also consider a longer time series constructed from all casts within a small region (<1 km<sup>2</sup>) at the intersection of these two lines, approximately 5.5 km from the river mouth (Figure 1).

## 4. Results

### 4.1. Plume and SSC Structure

[30] The near-field region of the Columbia plume is energetic and complex due to large tidal velocities and

substantial buoyancy input from the river [Jay *et al.*, 2008; Horner-Devine *et al.*, 2009]. In order to investigate the changes in plume structure and, in particular, the impact on plume sediment dynamics due to changes in river discharge we initially compare data from spring ebb tides in May 2006 (high flow) and August 2005 (low flow).

#### 4.1.1. High-Discharge, Spring Tide Period

[31] During the high-flow period in May 2006 the velocity and salinity structures of the ebb outflow extend to depths greater than 15 m only during the first half of the ebb and shoal rapidly after that (Figure 5, passes M1 and M2). During the latter half of the ebb the bottom current has reversed, drawing shelf water up toward the river mouth (Figure 5c). Throughout the ebb period most of the freshwater is carried in a strongly stratified near-surface layer that is <10 m deep. The plume stratification increases over the course of the ebb as the surface layer thins. At the end of ebb, the vertical density stratification in the plume, as measured by the buoyancy frequency, reaches 0.25 s<sup>-1</sup> (Figures 5i and 5j).

[32] The measurements of eddy diffusivity also suggest that the plume is decoupled from the bottom for most of the ebb in the high-flow period. Initially, eddy diffusivity is elevated ( $K_\rho > 10^{-3} \text{ m}^2 \text{ s}^{-1}$ ) throughout much of the water column at the landward end of the transect as the first pulse of ebb flow is discharged from the estuary (Figure 5, pass M1). However, the plume rapidly separates from the bottom and is completely decoupled midway through the ebb. Note that the diffusivity beneath the plume in the latter passes may be an overestimate due to the low stratification, as described in section 3.4. The bottom stress,  $\tau_b$ , is elevated on the landward end of the transect during the first half of the ebb, but is uniformly lower than 0.2 N m<sup>-2</sup> during the second half of the ebb (Figures 5u–5y).

[33] In the high-flow period, higher SSC is associated with the Columbia River outflow, and follows contours similar to those of fresher water and higher westward velocity (Figures 5a–5t). After the first pass, the SSC field separates vertically (Figures 5q–5t), displaying surface and bottom maxima. The layer of elevated SSC along the bottom is likely the result of sediment input on this tidal cycle, since no bottom sediment is observed along this transect earlier in the ebb despite high bottom stresses (Figures 5p and 5q). As noted above, bottom currents in latter part of the ebb are directed landward, suggesting that recently deposited sediment particles will be carried landward and may be trapped near the mouth or in the estuary.

#### 4.1.2. Low-Discharge, Spring Tide Period

[34] The velocity and salinity structure are markedly different during the low-discharge period. During the initial ebb both fields appear bottom attached (Figure 6a). A transition occurs in the plume structure between passes A2 and A3. After the transition the plume is detached from the bottom on the landward end of the transect but remains attached in the region between 5 and 7 km from the mouth (Figures 6c–6e). Seaward of the connection point, near-bottom water moves up-shelf, drawing deep salty water toward the attachment point (Figure 6c). This returning flow represents a possible pathway for marine sediments to be entrained into the plume. Landward of the attachment point the flow is uniformly seaward, resulting in a convergent flow along the bottom. Toward the end of the ebb the flow beneath the plume is directed landward and the surface plume has

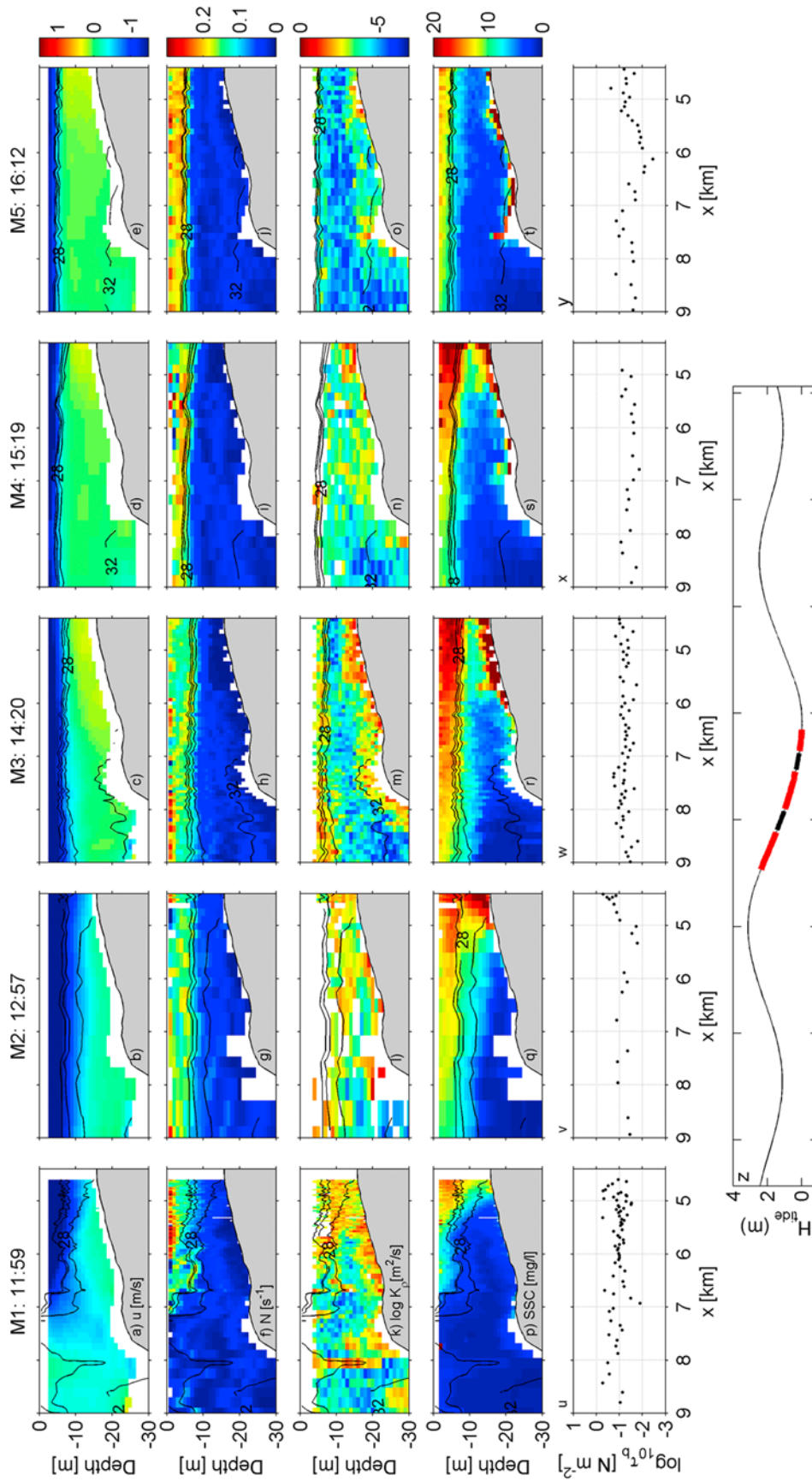


**Figure 5.** Hydrographic and sediment data from five transect passes during greater ebb spring study on 29 May 2006. Each pass in the sequence, which took approximately 1 h, is indicated at the top by M1 – M5 and the average time of the pass. The x axis represents along-transect distance from the river mouth. (a–e) E–W velocity (positive east), (f–j) buoyancy frequency, (k–o) the eddy diffusivity, (p–t) suspended sediment concentration, and (u–y) bottom stress. Salinity contours are repeated in each plot to indicate the structure of the plume. (z) Tidal height is plotted, and the times for each transect are indicated by the red and black sections.



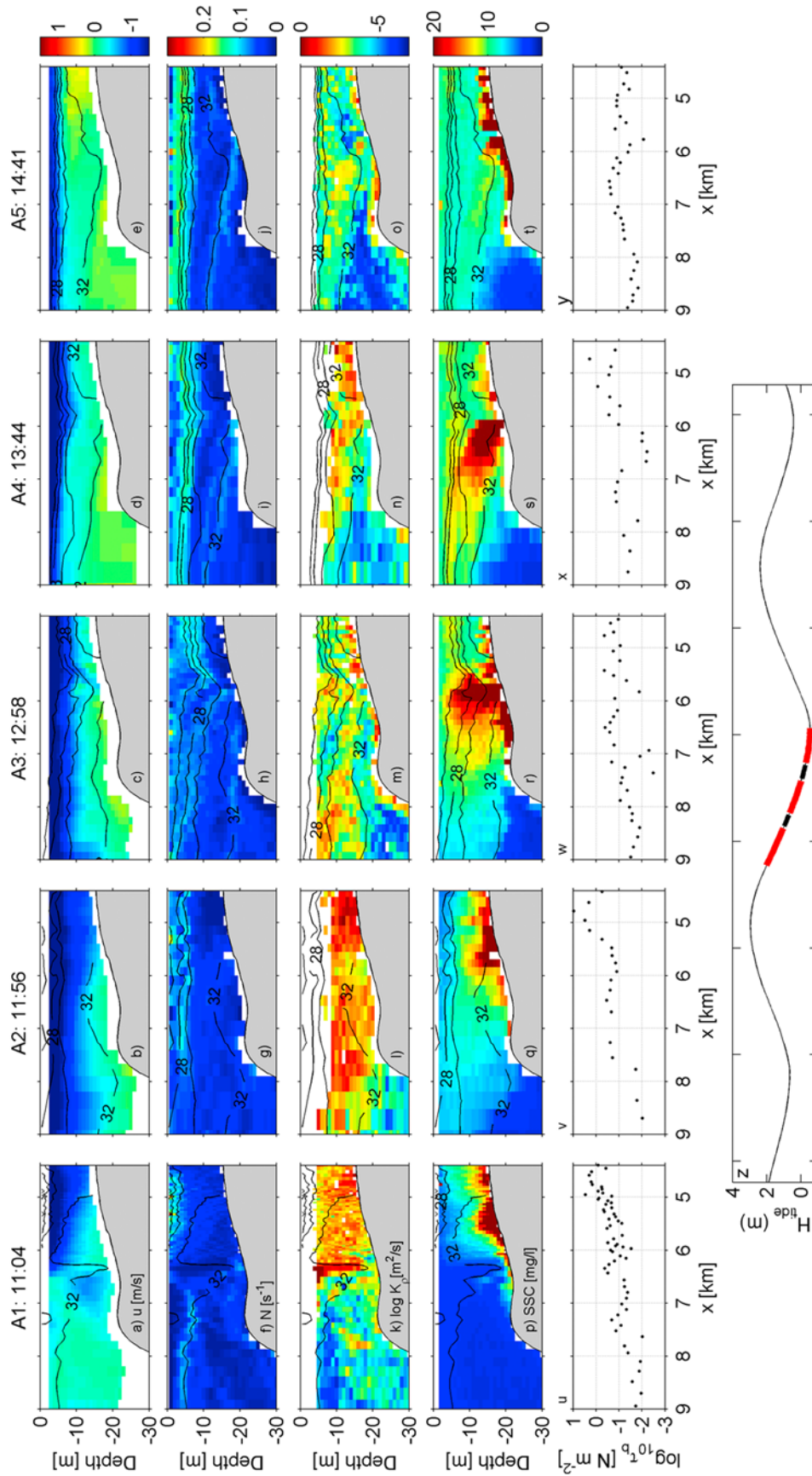


**Figure 6.** Hydrographic and sediment data from transect passes during greater ebb spring study on 20 August 2005. The plots are as in Figure 5. Each pass in the August sequence shown here is indicated at the top by A1–A5 and the average time of the pass.

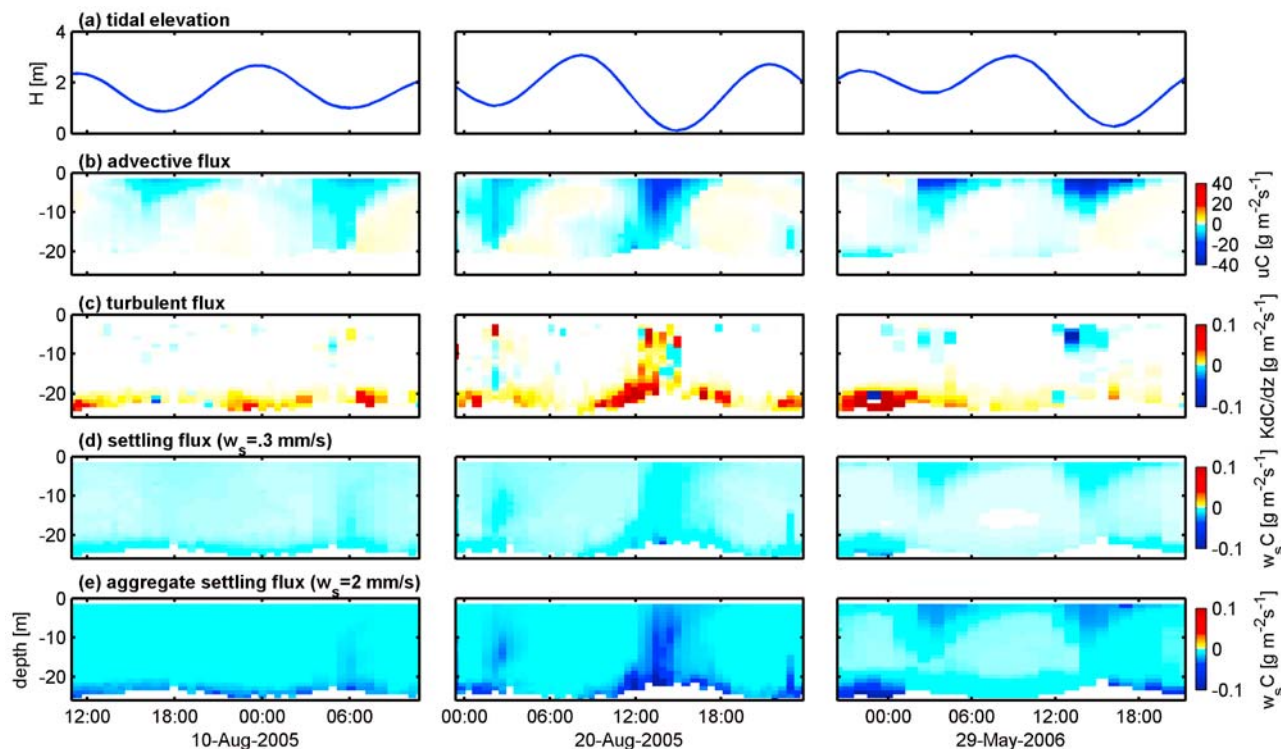


**Figure 7.** Flux time series based on data from  $x = 6$  km to  $x = 7.5$  km from the mouth during August neap (10 August 2005), August spring (20 August 2005), and May spring (29 May 2006). (a) Tidal elevation, (b) advective flux  $uC$ , (c) vertical turbulent flux  $K_{\rho}dC/dz$ , (d) particle settling flux  $w_sC$ , and (e) aggregate settling flux  $w_sC$ . The fall velocities used for the particle and aggregate settling fluxes are  $0.3 \text{ mm s}^{-1}$  and  $2.0 \text{ mm s}^{-1}$ , respectively.

become thinner and more stratified (Figure 6, pass A5). The buoyancy frequency is approximately  $0.15 \text{ s}^{-1}$ , however; significantly lower than the value in the high-flow period (Figures 6i and 6j).

[35] Throughout the ebb in the low-flow period, eddy diffusivities are elevated throughout the water column. On the first pass, at the beginning of the ebb, the eddy diffusivity spikes to values greater than  $10^{-1} \text{ m}^2 \text{ s}^{-1}$  within the initial density front and the bottom stress reaches values well above  $1 \text{ N m}^{-2}$ , more than an order of magnitude higher than the peak stresses in the high-flow period. Landward of the front, the region of elevated  $K_{\rho}$  extends uniformly from top to bottom with values greater than  $10^{-2} \text{ m}^2 \text{ s}^{-1}$ . In the final two passes near the end of the ebb, the turbulence is contained primarily in a structure that extends vertically and seaward from the bottom at the connection point. The peak bottom stresses decrease below  $1 \text{ N m}^{-2}$ , but remain an order of magnitude higher than the peak values observed during the same tidal phase in high-flow period.

[36] The combination of elevated water column turbulence and bottom stress, with convergent bottom velocity, generate a dynamic SSC field in August (Figures 6p–6t). The elevated bottom stress associated with the passage of the front and the initial ebb pulse resuspend sediment in the landward section of the transect (Figure 6). At the time of the transition, a large burst of sediment that extends almost to the water surface is observed at the location of the bottom connection point (Figure 6r). By the fourth and fifth passes it is clear that the

resuspended sediment is being entrained into the low-salinity surface plume and carried seaward. The sequence described here leading to resuspension into the upper water column is observed again on the EW line during the subsequent greater ebb on 21 August 2005.

#### 4.1.3. Low-Discharge, Neap Tide Period

[37] The structure of the ebb flow during neap tide periods is similar to that observed during the spring tides. However, significant sediment resuspension is only observed late in the ebb, after the transition to a partially attached plume, and the resuspended sediment is not observed to penetrate vertically quite as far into the water column. Due to the decrease in mixing early in the ebb, the plume is more stratified, and this stratification appears to limit the flux of sediment into the surface layers of the plume. Data from the low-flow neap period are presented in Figure 7 as part of the following sediment flux discussion.

#### 4.2. Sediment Fluxes

[38] In order to investigate the temporal variability and relative contribution of the dominant flux terms to the sediment dynamics in the near-field region, a time series of sediment flux data was generated by extracting transect data from the resuspension region between 6 and 7.5 km from the mouth (Figure 7). These data are used to compute the vertical turbulent flux ( $F_t = K_{\rho} dC/dz$ ), east-west advective flux ( $uC$ ), and settling flux ( $w_sC$ ), where  $C$  is used to denote the suspended sediment concentration. The advective flux is

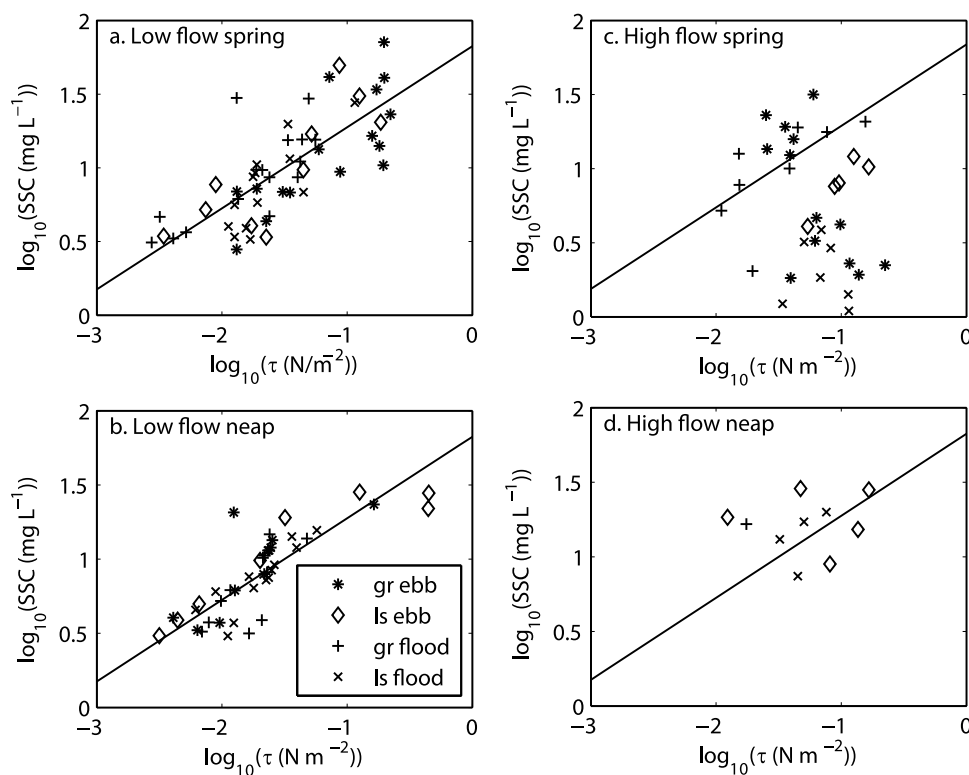


**Figure 8.** Near-bottom SSC versus bottom shear stress in a 0.5 km region 5.6 km from the mouth for spring and neap tides during (a, b) the August low-flow and (c, d) the May high-flow periods. The black line is the linear regression to the low-flow spring tide data, which is reproduced for comparison on the other plots.

much larger than the turbulent and settling fluxes, and not dynamically equivalent to the two vertical terms. Thus, the color axes are chosen to show the maximum contrast within each plot. The settling fluxes reported in Figure 7 represent the best available estimates of settling flux as described in section 3.3.

[39] During spring tide in the high-flow period only negative (downward) turbulent fluxes are observed in the upper water column (Figure 7, right). Near-surface turbulence is always associated with a positive upward gradient in sediment concentration, indicating downward transport of particles by turbulence. The highest settling fluxes are associated with the surface plume water and are strongly correlated with the advective flux. It is apparent that the primary source of sediment to the system is the river. The turbulent and settling fluxes have the same sign, and both remove sediment from the surface plume water. The maximum turbulent flux is equal to or larger than the particle settling flux on both ebbs and significantly exceeds the aggregate settling flux during the peak of the greater ebb. Although positive turbulent fluxes are observed near the bottom, they never penetrate higher than 5 m from the bottom. Thus, resuspension is limited to the near-bottom region and does not contribute to the plume sediment budget.

[40] In contrast to the high-flow conditions, the vertical turbulent sediment flux during spring tide in the low-flow period is almost entirely upward (positive) and penetrates from the bottom to the surface during the greater ebb (Figure 7, middle). The greatest turbulent flux occurs shortly after the middle of the ebb and the greatest upward penetra-

tion of sediment occurs just before lower low water. Advective flux appears to be associated with sediment that has been resuspended from the bottom as there is little sediment in the water column until resuspension occurs during greater ebb. This is consistent with Figures 6r and 6s, which also show higher suspended sediment concentrations from the bottom than from the estuary. During the greater ebb resuspension event, the turbulent flux exceeds the settling flux of fine particles and is approximately equal to the settling flux of aggregates. These flux estimates suggest that, during the low-discharge period in August, the primary source of sediment is the seabed, and that significant resuspension occurs primarily during strong ebbs. The resuspension is sufficient to deliver sediment high into the water column, where it is advected offshore by the surface flow. On the lesser ebb there is less vertical penetration and little sediment is entrained in the surface current.

[41] Sediment fluxes during the August neap study period (Figure 7, left) are significantly smaller than those during spring. They are limited primarily to the region within 5 m of the bottom and there is little upward or downward turbulent flux in the near-surface region.

#### 4.3. Bottom Stress

[42] The results described in sections 4.1 and 4.2 suggest that there may be a relationship between bottom shear stress ( $\tau_b$ ) and near-bottom SSC. The near-bottom SSC, defined as the average SSC value in the bottom 3 m, is plotted versus the corresponding  $\tau_b$  for the August spring tide, May spring tide, August neap tide and May neap tide in Figure 8. The SSC and

$\tau_b$  values in a 0.5 km region 5.6 km from the mouth were extracted and averaged for each transect, leading to one data point per transect in Figure 8.

[43] Two seasonal differences are apparent. First, there is a larger range in  $\tau_b$  in the high-flow period for both neap and spring tides; in the low-flow period,  $\tau_b$  varies over approximately 2 orders of magnitude compared with less than 1.5 in high-flow conditions. Second, there is a clear relationship between SSC and  $\tau_b$  in the low-flow period, but none during the high-flow period. A fit to the low-flow spring data gives a positive correlation between the logarithm of SSC and  $\tau_b$  with an  $r^2$  value of 0.6 (Figure 8a). The linear fit derived from the low-flow spring data also describes the variability in the low-flow neap data (Figure 8b), suggesting that the relationship is consistent across a range of tidal conditions.

[44] The near-bottom SSC data from spring tide in the high-flow period are more complex than during low flow (Figure 8c). Data from the lesser flood and some of the data from the greater ebb (these correspond to the beginning of the ebb) lie considerably below the line derived from the low-flow data. The observations suggest that resuspension in May is supply limited and that most of the sediment is delivered during the greater ebb. During the entire tidal cycle the bottom shear stress is relatively constant and sufficient to resuspend sediment. However, no significant suspended sediment is observed near bottom until midway through the greater ebb when it is resupplied from the estuary. After this time, elevated SSC continues through the greater flood and begins to diminish on the lesser ebb. During lesser flood, the amount of near-bottom SSC is an order of magnitude lower than during the greater flood; all of the fine sediment has been removed. It is likely that stormy weather preceding the spring period also helped to remove fine sediment from the shelf, so that no reserves were available (Figure 2).

[45] Although fewer data were acquired during the neap high-flow period, the limited data available suggest a slightly different story than during the spring high-flow period (Figure 8d). The neap data are all relatively close to the line from the low-flow SSC– $\tau_b$  relationship. This includes data from the lesser flood and lesser ebb, which all have SSC values considerably higher than the corresponding data from the spring tide period, indicating that the shelf never becomes supply limited. This may be because the supply of sediment from the estuary is better distributed over the entire tidal cycle.

#### 4.4. Entrainment of Sediment Into the Plume

[46] Since benthic sediment is known to contain nutrients and micronutrients valuable to the marine ecosystem, the impact of the resuspension observed during low-flow conditions in August will depend on whether or not the resuspended sediment is entrained into the surface plume, settles back to the bottom, or is otherwise removed offshore. In Figure 9, the vertical turbulent sediment fluxes are averaged by salinity class, based on data from the five ebb transects shown in Figures 5 and 6. At salinities between 31 and 33, positive fluxes are observed in both low- and high-flow conditions. In the range between 23 and 31, large positive and negative fluxes are observed for low flows. This latter range of salinities spans the range observed on the interface between the plume and the shelf water. Combined with the

fact that the freshest water is observed at the surface, these positive fluxes are indicative of sediment flux into the fresher plume water. By comparison, the turbulent sediment fluxes are almost entirely negative in this interfacial salinity class in the high-flow period, confirming that the flux is out of the plume.

#### 4.5. Control of Vertical Sediment Flux

[47] The results in sections 4.1–4.4 suggest that resuspension and entrainment of sediment into the plume is much greater during the low-flow period than the high-flow period. Here we suggest these differences are associated with changes in physical forcing (the competition between mixing and river flow), with a secondary effect from seasonal changes in sediment supply. Although sampling during the low-flow period occurred during slightly stronger tides, the most pronounced difference between the two periods is the delivery of freshwater from the river (Figures 10a and 10e). The importance of freshwater supply in controlling the structure and composition of the river plume is explored by *Nash et al.* [2009]. It is found that the composition (i.e., dilution) of river water leaving the estuary is set by the ratio between tidally generated bottom turbulence and freshwater river flow, which they characterize using the estuary Richardson number [*Fischer, 1972*]:

$$Ri_E = \frac{g'Q}{bu_{tidal}^3}.$$

Here  $g'$  is the reduced gravity representing the density anomaly between the river water and the ambient ocean water and  $b$  is the width of the channel at the river mouth. *Nash et al.* [2009] interpret  $Ri_E$  as the ratio between freshwater transport (per unit width;  $Q/b$ ) and the tidal power available for turbulent mixing ( $u_{tidal}^3$ ). Both plume freshness (or dilution) and plume thickness scale with  $Ri_E$ , such that highly stratified, surface-trapped plumes form during periods of high  $Ri_E$ , whereas more weakly stratified, bottom-reaching plumes are associated with low  $Ri_E$ . These differences in plume structure are evident in the transect data presented in Figures 5 and 6; the plume structure as evidenced by the isohalines penetrates considerably deeper during the low-flow period. Because turbulence in the near-field region is primarily driven by shear at the base of the tidal plume, shallow plumes (i.e., high  $Ri_E$ ) generally produce weaker near-bottom turbulence and stress.

[48] In the following, we examine the low-frequency variability in forcing and turbulent fluxes by computing bin averages over 24.8 h, thus masking effects associated with the diurnal inequality. In Figure 10 the tidal daily averaged (24.8 h) vertical sediment flux is compared to variables thought to influence resuspension, including the river discharge  $Q$ , the tidal forcing  $u_{tidal}$ , the wave-generated bottom stress  $\tau_w$  and the measured near-bottom stress  $\tau_b$ . The sediment flux values correspond to the midwater column, 4–5 mab, which is generally above the bottom boundary layer and beneath the plume. This measure is intended to represent the flux out of the boundary layer and into the plume. Following *Nash et al.* [2009], the amplitude of the tidal forcing is quantified in terms of the RMS tidal velocity as estimated at Station E using the CORIE simulation

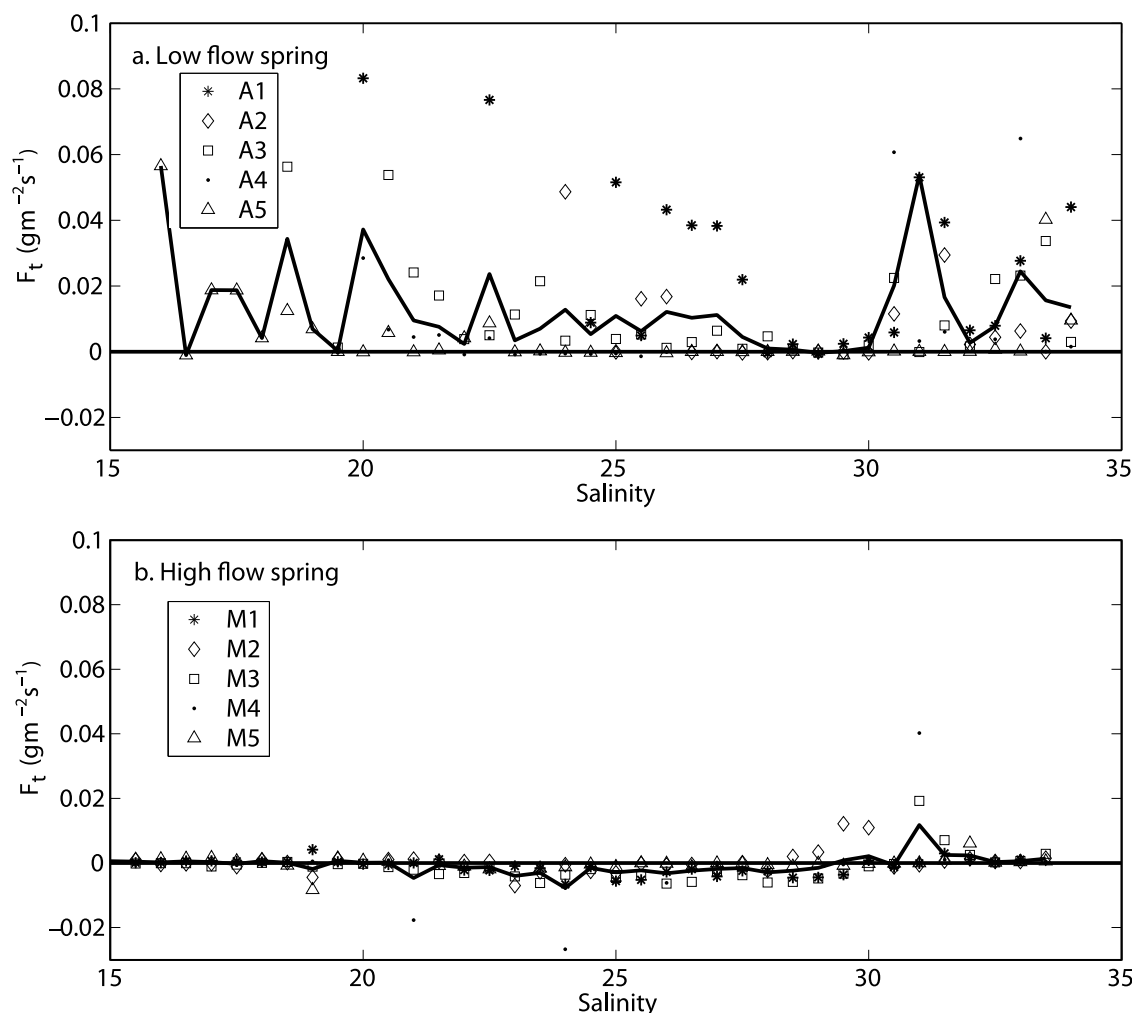


**Figure 9.** Vertical turbulent sediment flux plotted versus salinity for five transects in the low-flow period (August 2005) and the high-flow period (May 2006). The transects are the same as those shown in the Figures 5 and 6. The black line, which is the average turbulent flux in each salinity class, indicates that flux in intermediate plume salinity classes is upward and into the plume in low-flow conditions but is downward and out of the plume in high-flow conditions.

database [Baptista, 2006] and smoothed over a 24.8 h period to capture daily time scale variability. For calculation of sediment flux and bottom stress we consider data from the EW transect as well as data from a repeated NS transect. We generate a time series from all casts within a small region (<1 km<sup>2</sup>) at the intersection of these two lines, approximately 5.5 km from the river mouth (Figure 1). The time series from both years span a range of tidal amplitudes, wave conditions and river discharge rates.

[49] Daily averaged values of vertical turbulent sediment flux  $F_t$  in the midwater column for the high- and low-flow periods display two primary trends (Figures 10c and 10g): (1) the observed fluxes are significantly larger during the low-flow period (the average observed flux is more than ten times larger in 2005 compared with 2006) and (2) during the low-flow period, flux is much higher during spring tide when  $u_{\text{tidal}}$  is high. It is important to note that the value of  $F_t$  on 23 August 2005 is significantly higher than all the other observed values ( $F_t = 0.066 \text{ g}^{-2} \text{ s}^{-1}$ ). However, it is consistent with the trend from the other days in that it corresponds to a

day with high  $u_{\text{tidal}}$  and relatively low  $Q$ . Also note that the resuspension event documented in Figure 6 on 20 August 2005 only corresponds to an average daily sediment flux for that period.

[50] According to the observations above,  $F_t$  generally increases with  $u_{\text{tidal}}$  and decreases with  $Q$ . This is consistent with the hypothesis that the vertical flux of sediment is controlled by the competition between turbulence and vertical density stratification. Indeed, large resuspension events that carry sediment out of the bottom boundary layer are associated with conditions in which the gradient Richardson number  $Ri_g = N^2/u_z^2$  is less than 0.25 (not shown).

[51] The estuary Richardson number  $Ri_E$ , smoothed with a 24.8 h window, is plotted for the low- and high-flow periods in Figures 10d and 10h, respectively.  $Ri_E$  shows a clear spring-neap variation in both years and is significantly lower during the low-flow spring tide due to reduced buoyancy input. The magnitude of  $F_t$  agrees with the variation in  $Ri_E$ , especially during the low-flow period. In Figure 11, daily averaged flux at 4–5 mab is plotted versus  $Ri_E$  for both

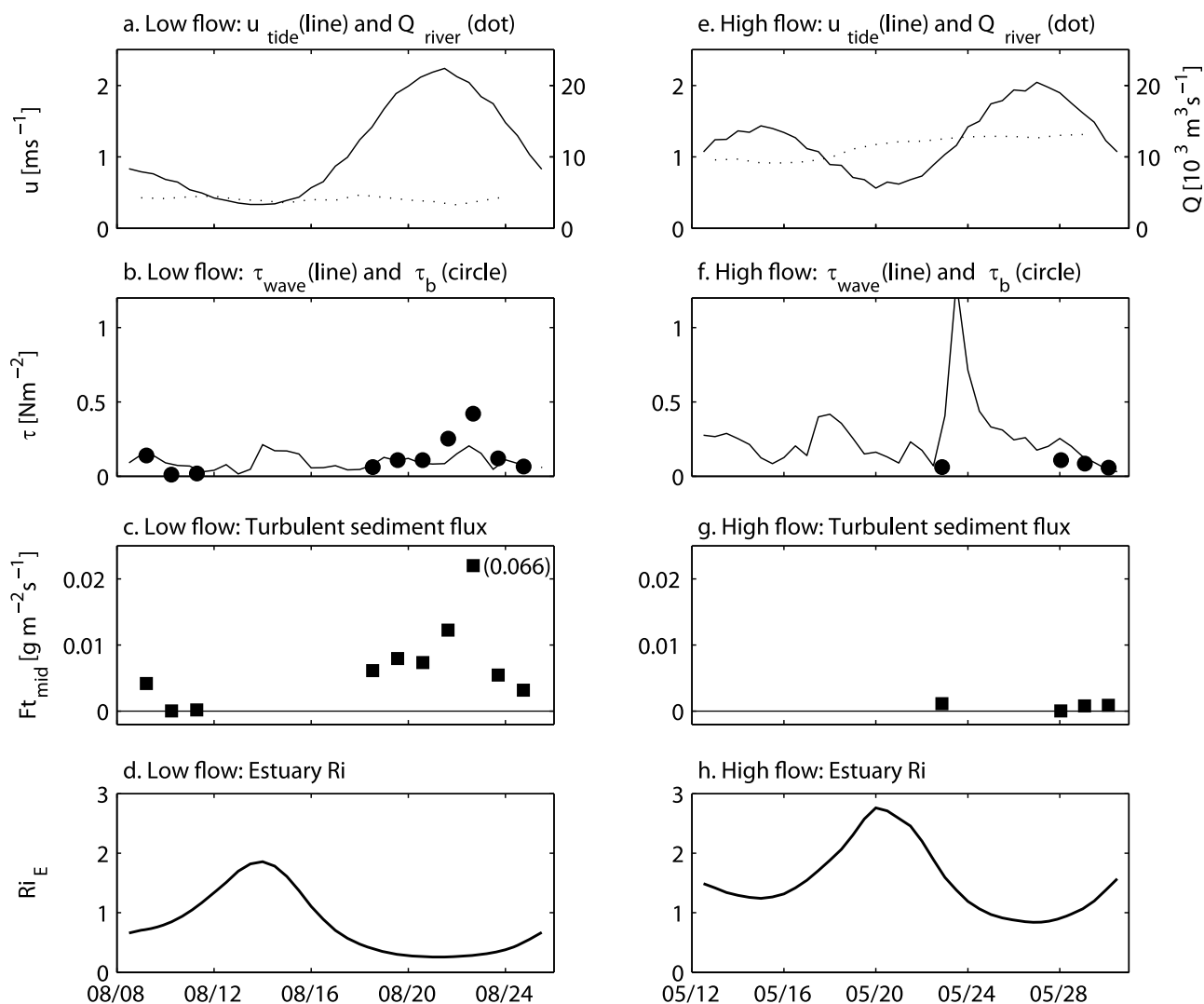


**Figure 10.** Comparison of forcing parameters with vertical turbulent sediment fluxes during (a–d) the low-flow period in 2005 and (e–h) the high-flow period in 2006. RMS tidal velocity and Columbia River discharge (Figures 10a and 10e), wave and daily averaged bottom shear stresses (Figures 10b and 10f), daily averaged vertical turbulent sediment fluxes in the midwater column (4–5 mab) (Figures 10c and 10g), and 24 h smoothed estuary Richardson number (Figures 10d and 10h). Note that the sediment flux on 23 August 2005 far exceeds all other observed values ( $F_t = 0.066 \text{ g}^{-2} \text{ s}^{-1}$ ).

periods.  $Ri_E$  appears to have reasonably good ability for predicting resuspension in this region. During the low-flow period, sediment flux decreases with increasing  $Ri_E$ . Throughout the high-flow sampling period  $Ri_E$  was higher than during the low-flow period and higher than 0.6, and the sediment flux was correspondingly low. Taken together, these data suggest that significant resuspension occurs when  $Ri_E < 0.6$ ; the average  $F_t$  was more than an order of magnitude larger for  $Ri_E < 0.6$  compared with  $Ri_E > 0.6$ . A very similar dependence is observed when midwater column SSC is plotted versus  $Ri_E$  (not shown), confirming that this result is independent of our parameterization of the sediment diffusivity.

[52] The processes of resuspension and entrainment of bottom sediment into the plume requires three conditions to be met: (1) bottom stress must be sufficient to resuspend sediment, (2) water column turbulence or vertical advective processes must be energetic enough to transport the sediment vertically through the water column, and (3) sufficient

sediment must be available on the seabed. The dependence on  $Ri_g$  and  $Ri_E$  described above suggests that the second condition provides an important control on the vertical sediment flux into the plume. *Nash et al.* [2009] find that plume thickness  $h_{plume}$  is related to  $Ri_E$ ; lower  $Ri_E$  results in a thicker plume. Thus,  $Ri_E$  also determines the degree of interaction of the plume with the seabed, providing increased bottom stress when  $Ri_E$  is low.

[53] The daily averaged bottom stress and 24.8 h smoothed wave stress are plotted in Figures 10b and 10f. During the low-flow period, bottom stress is inversely correlated with  $Ri_E$  and with sediment flux  $F_t$ . It is not clear from this comparison whether high turbulence intensities observed in the water column are the result of local boundary generated turbulence, or elevated bed stresses are the result of turbulent processes originating landward of our sampling location that are impacting the seabed. It is evident from the differences in plume structure documented in Figures 5 and 6, however, that

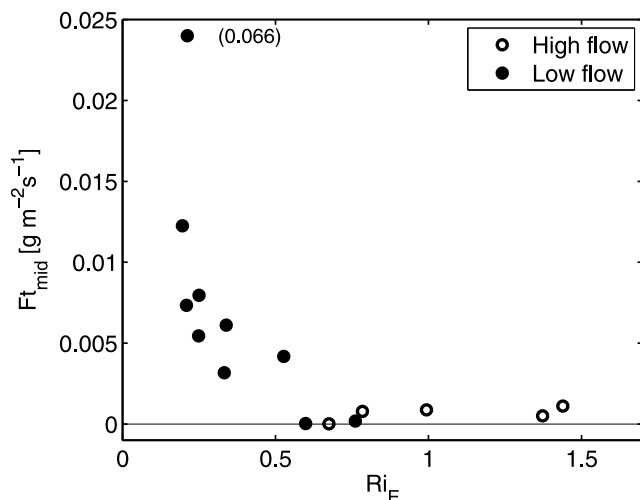


**Figure 11.** Daily averages of vertical turbulent sediment flux in the midwater column (4–5 mab) versus estuary Richardson number for all data in high- (2006) and low- (2005) flow periods. As in Figure 10, one sediment flux value is off scale.

less stratified conditions lead to stronger coupling between surface and bottom processes. Thus, the elevated water column turbulence and bottom stress are expected to cooccur during the low-flow period. Bottom stress and  $F_t$  do not show sufficient variability during the high-flow period to deduce any clear relationship.

[54] There is a weak relationship between wave stress and vertical sediment flux  $F_t$  in the low-flow period and no relationship during the high-flow period. However, sampling during the high-flow period was interrupted by a large storm on 23–28 May 2006 that generated wave stresses far exceeding any other time during our sampling. These almost certainly caused significant resuspension of bottom sediment and possibly eroded any fine sediment previously deposited on the shelf. It is difficult to isolate the relative roles of

decreased sediment supply and increased stratification (high  $Ri_E$ ) in producing low sediment flux. However, both appear to be important and both provide for more resuspension of bottom sediment in the low-flow period compared with the high-flow period.

## 5. Discussion

[55] The observations outlined above describe two different sediment transport regimes in the near-field region of the Columbia River plume system, which occur during low and high river flow periods corresponding to late summer (August 2005) and late spring (May 2006). The sediment dynamics that are observed during a large ebb in the high-flow period are summarized in the schematic in Figure 12a. The plume is strongly stratified and, after the initial ebb pulse, thins rapidly and loses contact with the bottom in this region of the shelf. From this point on, the flow is directed landward along the bottom. More sediment is carried in the plume in the high-flow period compared with the low-flow period, and that sediment appears to come directly from the estuary. Mixing and gravitational flux act to detrain sediment from the plume as it evolves seaward. Resuspension is limited to the bottom 5 m and there is no direct flux of benthic sediment into the plume. The sediment dynamics that are observed during ebb in the low-flow period are very different (Figure 12b). During the spring tide large resuspension events are observed, which mobilize bottom sediments and mix them upward into the water column. Observations of advective flux in the near-surface region and salinity-binned turbulent flux confirm that the resuspended sediments are entrained into the fresher surface plume water, where they are transported rapidly away from the river mouth.

[56] During the low-flow period, resuspension, measured as vertical turbulent sediment flux  $F_b$ , was correlated with estuary Richardson number  $Ri_E$ ; sediment flux was small for  $Ri_E > 0.6$  and increased by more than an order of magnitude for  $Ri_E \sim 0.2$  (Figure 11). During the high-flow period  $Ri_E$  was always greater than 0.6 and sediment flux was consis-

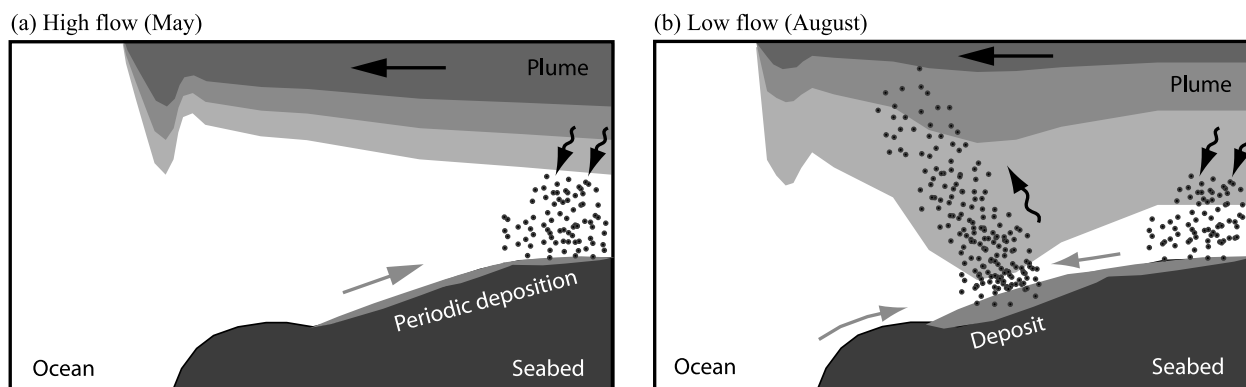


**Figure 12.** Conceptual schematics showing the different hydrodynamic and sediment transport regimes observed in (a) high-flow (May) and (b) low-flow (August) conditions during spring ebb tide. Black arrows indicate flow of surface plume water, gray arrows indicate near-bottom flow, and wavy arrows indicate dominant exchanges of sediment between the plume and the seabed. In low- and high-flow conditions sediment is lost from the plume due to gravitation settling and turbulent mixing. In low-flow conditions, contact between the plume and the seabed also causes significant upward flux of sediment that is entrained into the plume.

tently low. Although the measured sediment fluxes during the high-flow period are consistent with the trend in the low-flow period, no relationship was observed within the high-flow period between sediment flux and  $Ri_E$ .

[57] It is very likely that observations of  $F_t$  during high-flow conditions were also affected by decreased sediment supply on the seabed, which has been shown to have considerable seasonal variability. *Nittrouer and Sternberg* [1981] observed a thin deposit of fine sediments on the shelf in August, which overlay a thicker layer of medium-grained sand. This is consistent with our observations from August. In a separate survey during the winter, *Nittrouer and Sternberg* [1981] found that the silt layer was absent; leading them to conclude that winter storms removed the sediment. Thus, the majority of the fine sediments observed on the shelf during the summer must be deposited during the spring freshet, when storm waves had decreased and sediment loading from the river is high.

[58] The high-flow sampling period followed closely after a series of spring storms that were associated with high wave stresses (Figure 2d). As a result, it appears that there was no bottom deposit in the near-field region to provide a consistent supply of fine sediment for resuspension; the observed  $F_t$  was the result of sediment delivered to the seabed within the same tidal cycle. Our observation that low sediment flux is associated with high  $Ri_E$  during the high-flow period is due in part to the inconsistent supply of sediment on the seabed in this region. Nonetheless, the dramatic differences in water column structure between the low- and high-flow periods suggest that, even if there were no supply limitation, sediment resuspended in the high-flow conditions is much less likely to be entrained into the plume in the manner observed for the low-flow period.

[59] The relationship between  $F_t$  and  $Ri_E$  observed during the low-flow period in August suggests that, when there is sufficient supply of sediment on the seabed, the resuspension of sediment into the plume depends on the competition between the stratification provided by river buoyancy input and tidally generated turbulence. In particular, low  $Ri_E$  leads to a thicker plume [*Nash et al.*, 2009] and more interaction with the bottom. Since  $Ri_E$  is derived from easily accessible parameters, namely river discharge and tidal velocity, this relationship presents an opportunity to predict the magnitude and timing of resuspension events during spring and summer. It is clear from Figures 10 and 11 that tidally generated turbulence is not sufficient to cause significant resuspension during neap tides even in low-flow conditions. During high-flow conditions, however, even modest spring tides do not result in low-enough  $Ri_E$  for resuspension to be predicted. In order to generate an improved prediction for the resuspension of bottom sediment in to the plume, however, it is clear that a better understanding of the seasonal variation in the near-field fine sediment deposit is required. Measurements under a wider variety of conditions are needed.

[60] The importance of plume fine sediment transport is related to the nutrients and micronutrients that are carried with them [*Lohan and Bruland*, 2006]. An important consequence of the resuspension described above is that it makes sediment and nutrients available during spring and summer to the plume-supported ecosystem. Resuspension of sediment in the bottom boundary layer such as that observed in the May high-flow period has less relevance to the plume

ecosystem than the large resuspension events observed during the August low-flow period, which reentrain fine sediment from the bottom into the plume and make sediment-associated nutrients available. Additionally, since micronutrients such as iron may be transformed into more bioavailable states when they are retained in benthic sediments, cycles in which they are trapped, deposited and resuspended may increase their contribution to the marine ecosystem in a manner roughly analogous to that observed in an estuarine ETM [e.g., *Simenstad et al.*, 1995].

[61] Marine chemistry data collected during the RISE cruises in the near-field plume region indicate that during May 2006, the iron originates from a river source, compared to August 2005 when it comes from a marine source [*Lohan and Bruland*, 2006]. Iron measurements also indicate a strong tidal and spring-neap variability. They suggest that the benthic supply of iron from sediments outside the river mouth is of equal importance to the supply from the river. In particular, the fraction of total dissolved iron due to iron II was observed to be highest at the end of ebb tide and during spring tides [*Lohan and Bruland*, 2006]. This observation is consistent with the seasonal and tidal variation observed in the sediment dynamics. Micronutrient observations also indicate that the dissolved manganese concentration depends strongly on the tides and may be higher in the plume near field than in the surface ocean water or in the estuary [*Aguilar-Islas and Bruland*, 2006]. This is consistent with the findings of *Klinkhammer et al.* [1997], who observed high manganese gradients and turbidity at the seaward front of the Columbia plume. In addition to incorporation of upwelled fluid, the observations suggest that there is a benthic source in this region. Both of the iron and manganese observations highlight the potential role of near-field resuspension in the plume biological system.

[62] **Acknowledgments.** The authors would like to thank R. Kreth and A. Perlin for their technical expertise and Jay Peterson and Keith Leffler for additional help on the cruises. We also thank Captain Ron L. Short of the R/V *Point Sur* and marine technicians Stewart Lamberdin, Christina Courcier, and Ben Jokinen for their superb support of in situ data collection. The research was funded by the University of Washington Royalty Research Fund and the National Science Foundation (River Influences on Shelf Ecosystems OCE 0239072 and OCE 0648655). This is RISE publication 36.

## References

- Aguilar-Islas, A. M., and K. W. Bruland (2006), Dissolved manganese and silicic acid in the Columbia River plume: A major source to the California Current and coastal waters off Washington and Oregon, *Mar. Chem.*, *101*, 233–247, doi:10.1016/j.marchem.2006.03.005.
- Baptista, A. (2006), CORIE: The first decade of a coastal-margin collaborative observatory, in *Oceans 2006*, pp. 1–6, Inst. of Electr. and Electr. Eng., Boston, Mass.
- Bogucki, D., T. Dickey, and L. G. Redekopp (1997), Sediment resuspension and mixing by resonantly generated internal solitary waves, *J. Phys. Oceanogr.*, *27*, 1181–1196, doi:10.1175/1520-0485(1997)027<1181:SRAMBR>2.0.CO;2.
- Bottom, D. L., C. A. Simenstad, J. Burke, A. M. Baptista, D. A. Jay, K. K. Jones, E. Casillas, and M. H. Schiewe (2005), Salmon at river's end: The role of the estuary in the decline and recovery of Columbia River salmon, *NOAA Tech. Memo. NMFS-NWFSC-68*, 246 pp., U.S. Dep. of Commer., NOAA, Washington, D. C.
- Boyle, E. A., J. M. Edmond, and E. R. Sholkovitz (1977), The mechanism of iron removal in estuaries, *Geochim. Cosmochim. Acta*, *41*, 1313–1324, doi:10.1016/0016-7037(77)90075-8.
- Bruland, K. W., E. L. Rue, and G. J. Smith (2001), Iron and macronutrients in California coastal upwelling regimes: Implications for diatom blooms, *Limnol. Oceanogr.*, *46*(7), 1661–1674.



- Bruland, K. W., M. C. Lohan, A. M. Aguilar-Islas, G. J. Smith, B. Sohst, and A. Baptista (2008), Factors influencing the chemistry and formation of the near-field Columbia River plume: Nitrate, silicic acid, dissolved Fe, and dissolved Mn, *J. Geophys. Res.*, *113*, C00B02, doi:10.1029/2007JC004702.
- Chase, Z., P. G. Stratton, and B. Hales (2007), Iron links river runoff and shelf width to phytoplankton biomass along the U.S. West Coast, *Geophys. Res. Lett.*, *34*, L04607, doi:10.1029/2006GL028069.
- Chisholm, T. A., and D. A. Jay (2004), Columbia River suspended sediment monitoring, *Eos Trans. AGU*, *85*(47), Fall Meet. Suppl., Abstract H11F-0377.
- Conomos, T. J., M. G. Groos, C. A. Barnes, and F. A. Richards (1972), River-ocean nutrient relations in summer, in *The Columbia River Estuary and Adjacent Ocean Waters*, edited by A. T. Pruter and D. L. Alverson, pp. 151–175, Univ. of Wash. Press, Seattle.
- Dagg, M., R. Benner, S. Lohrenz, and D. Lawrence (2004), Transformation of dissolved and particulate materials on continental shelves influenced by large rivers: Plume processes, *Cont. Shelf Res.*, *24*(7–8), 833–858, doi:10.1016/j.csr.2004.02.003.
- Fain, A. M. V., D. A. Jay, D. J. Wilson, and A. M. Baptista (2001), Seasonal and tidal monthly patterns of particulate matter dynamics in the Columbia River estuary, *Estuaries*, *24*(5), 770–786, doi:10.2307/1352884.
- Fischer, H. B. (1972), Mass transport mechanisms in partially stratified estuaries, *J. Fluid Mech.*, *53*, 671–687.
- Geyer, W. R., P. S. Hill, and G. C. Kineke (2004), The transport, transformation and dispersal of sediment by buoyant coastal flows, *Cont. Shelf Res.*, *24*(7–8), 927–949, doi:10.1016/j.csr.2004.02.006.
- Grant, W. D., and O. S. Madsen (1979), Combined wave and current interaction with a rough bottom, *J. Geophys. Res.*, *84*, 1797–1808.
- Hickey, B. M., L. J. Pietrafesa, D. A. Jay, and W. C. Boicourt (1998), The Columbia River plume study: Subtidal variability in the velocity and salinity fields, *J. Geophys. Res.*, *103*, 10,339–10,368, doi:10.1029/97JC03290.
- Hickey, B. M., et al. (2009), River influences on shelf ecosystems: Introduction and synthesis, *J. Geophys. Res.*, doi:10.1029/2009JC005452, in press.
- Hill, P. S., T. G. Milligan, and W. R. Geyer (2000), Controls on effective settling velocity of suspended sediment in the Eel River flood plume, *Cont. Shelf Res.*, *20*(16), 2095–2111, doi:10.1016/S0278-4343(00)00064-9.
- Horner-Devine, A. R., D. A. Jay, P. M. Orton, and E. Y. Spahn (2009), A conceptual model of the strongly tidal Columbia River plume, *J. Mar. Syst.*, *78*, 460–475, doi:10.1016/j.jmarsys.2008.11.025.
- Jay, D. A., E. D. Zaron, and J. Pan (2008), Initial expansion of the Columbia River tidal plume: Theory and remote sensing observations, *J. Geophys. Res.*, doi:10.1029/2008JC004996, in press.
- Johnson, K. S., F. P. Chavez, and G. E. Friederich (1999), Continental-shelf sediment as a primary source of iron for coastal phytoplankton, *Nature*, *398*, 697–700, doi:10.1038/195111.
- Klinkhammer, G. P., C. S. Chin, C. Willson, M. D. Rudnicki, and C. R. German (1997), Distributions of dissolved manganese and fluorescent dissolved organic matter in the Columbia River estuary and plume as determined by in situ measurement, *Mar. Chem.*, *56*, 1–14, doi:10.1016/S0304-4203(96)00079-5.
- Landry, M. R., J. R. Postel, W. K. Peterson, and J. Newman (1989), Broad-scale distributional patterns of hydrographic variables on the Washington/Oregon shelf, in *Coastal Oceanography of Washington and Oregon*, edited by M. Landry and B. M. Hickey, pp. 1–40, Elsevier, Amsterdam.
- Lohan, M. C., and K. W. Bruland (2006), Importance of vertical mixing for additional sources of nitrate and iron to surface waters of the Columbia River plume: Implications for biology, *Mar. Chem.*, *98*, 260–273, doi:10.1016/j.marchem.2005.10.003.
- McKee, B. A., R. C. Aller, M. A. Allison, T. S. Bianchi, and G. C. Kineke (2004), Transport and transformation of dissolved and particulate materials on continental margins influenced by major rivers: Benthic boundary layer and seabed processes, *Cont. Shelf Res.*, *24*(7–8), 899–926, doi:10.1016/j.csr.2004.02.009.
- Mikkelsen, O. A., and M. Pejrup (2001), The use of a LISST-100 laser particle sizer for in-situ estimates of floc size, density and settling velocity, *Geo Mar. Lett.*, *20*, 187–195, doi:10.1007/s003670100064.
- Mikkelsen, O. A., T. G. Milligan, P. S. Hill, R. J. Chant, C. F. Jago, S. E. Jones, V. Krivtsov, and G. Mitchelson-Jacob (2008), The influence of schlieren on in situ optical measurements used for particle characterization, *Limnol. Oceanogr. Methods*, *6*, 133–143.
- Milliman, J. D., and J. P. M. Syvitski (1992), Geomorphic/tectonic control of sediment discharge to the ocean: The importance of small mountainous rivers, *J. Geol.*, *100*(5), 525–544, doi:10.1086/629606.
- Moum, J., M. Gregg, R. Lien, and M. Carr (1995), Comparison of turbulence kinetic energy dissipation rate estimates from two ocean microstructure profilers, *J. Atmos. Oceanic Technol.*, *12*, 346–366, doi:10.1175/1520-0426(1995)012<0346:COTKED>2.0.CO;2.
- Nash, J. D., and J. N. Moum (2005), River plumes as a source of large-amplitude internal waves in the coastal ocean, *Nature*, *437*, 400–403, doi:10.1038/nature03936.
- Nash, J., L. Kilcher, and J. Moum (2009), Structure and composition of a strongly stratified, tidally pulsed river plume, *J. Geophys. Res.*, *114*, C00B12, doi:10.1029/2008JC005036.
- Nittrouer, C. A., and R. W. Sternberg (1981), The formation of sedimentary strata in an allochthonous shelf environment: The Washington continental shelf, *Mar. Geol.*, *42*(1–4), 201–232, doi:10.1016/0025-3227(81)90164-X.
- Orton, P. M., and D. A. Jay (2005), Observations at the tidal plume front of a high-volume river outflow, *Geophys. Res. Lett.*, *32*, L11605, doi:10.1029/2005GL022372.
- Osborn, T. R. (1980), Estimates of the local rate of vertical diffusion from dissipation measurements, *J. Phys. Oceanogr.*, *10*, 83–89, doi:10.1175/1520-0485(1980)010<0083:EOTLRO>2.0.CO;2.
- Perlin, A., J. N. Moum, J. M. Klymak, M. D. Levine, T. Boyd, and P. M. Kosro (2005), A modified law-of-the-wall applied to oceanic bottom boundary layers, *J. Geophys. Res.*, *110*, C10S10, doi:10.1029/2004JC002310.
- Reed, D. J., and J. Donovan (1994), The character and composition of the Columbia River estuarine turbidity maximum, in *Changes in Fluxes in Estuaries*, edited by K. R. Dyer and R. J. Orth, pp. 445–450, Olsen and Olsen, Fredensborg, Denmark.
- Rose, C. P., and P. D. Thorne (2001), Measurements of suspended sediment transport parameters in a tidal estuary, *Cont. Shelf Res.*, *21*(15), 1551–1575, doi:10.1016/S0278-4343(00)00087-X.
- Simenstad, C. A., D. Reed, D. A. Jay, F. Prahl, L. Small, and J. A. Baross (1995), LMER in the Columbia River estuary: An interdisciplinary approach to investigating couplings between hydrological, geochemical and ecological processes, in *Changing Particle Fluxes in Estuaries: Implications From Science to Management*, edited by K. R. Dyer and R. J. Orth, pp. 437–444, Olsen and Olsen, Fredensborg, Denmark.
- Souza, A. J., L. G. Alvarez, and T. D. Dickey (2004), Tidally induced turbulence and suspended sediment, *Geophys. Res. Lett.*, *31*, L20309, doi:10.1029/2004GL021186.
- Styles, R. (2006), Laboratory evaluation of the LISST in a stratified fluid, *Mar. Geol.*, *227*(1–2), 151–162, doi:10.1016/j.margeo.2005.11.011.
- Sullivan, B. E., F. G. Prahl, L. F. Small, and P. A. Covert (2001), Seasonality of phytoplankton production in the Columbia River: A natural or anthropogenic pattern?, *Geochim. Cosmochim. Acta*, *65*, 1125–1139, doi:10.1016/S0016-7037(00)00565-2.
- Tragou, E., V. Zervakis, E. Papageorgiou, S. Stavrakakis, and V. Lykousis (2005), Monitoring the physical forcing of resuspension events in the Thermaikos Gulf—NW Aegean during 2001–2003, *Cont. Shelf Res.*, *25*(19–20), 2315–2331.
- van Rijn, L. C. (1984), Sediment transport, Part II: Suspended load transport, *J. Hydrol. Eng.*, *110*(11), 1613–1641.
- Wiberg, P. L., D. E. Drake, and D. A. Cacchione (1994), Sediment resuspension and bed armoring during high bottom stress events on the northern California inner continental shelf: Measurements and predictions, *Cont. Shelf Res.*, *14*(10–11), 1191–1219, doi:10.1016/0278-4343(94)90034-5.
- Wright, L. D., and C. A. Nittrouer (1995), Dispersal of river sediments in coastal seas: Six contrasting cases, *Estuaries*, *18*(3), 494–508, doi:10.2307/1352367.

A. R. Horner-Devine and E. Y. Spahn, Department of Civil and Environmental Engineering, University of Washington, Seattle, WA 98195, USA. (arhd@u.washington.edu)

D. A. Jay, Department of Civil and Environmental Engineering, Portland State University, Portland, OR 97207, USA.

L. Kilcher and J. D. Nash, College of Oceanic and Atmospheric Sciences, Oregon State University, Corvallis, OR 97331, USA.